Desalination and Water Treatment
www.deswater.com

doi: 10.1080/19443994.2013.800279

52 (2014) 3347–3354
April

Taylor & Francis
Taylor & Francis Group

Effect of liquid phase physicochemical characteristics on hydrodynamics of an electroflotation column

I. Ksentini, M. Kotti, L. Ben Mansour*

Research Unit of Applied Fluid Mechanics and Modeling, Sciences Faculty of Sfax, University of Sfax, B.P.1171, Sfax 3000, Tunisia
Tel. +216 98 657 061; Fax: +216 74 666 479; email: lassaadbenmansour@yahoo.fr

Received 20 June 2012; Accepted 22 April 2013

ABSTRACT

The objective of this work is to study the effect of the liquid phase physicochemical characterization on the hydrodynamic parameters of an electroflotation column working in batch mode. Video recording and image processing method was employed to calculate the oxygen bubbles diameter and velocity, as well as gas holdup. Tap water, a solution of cationic surface tension as well as a solution of anionic surface tension have been used as model solutions in order to evaluate the viscosity and the surface tension effect on oxygen bubble parameters and gas holdup. Models predicting bubble diameters, Reynolds number, and gas holdup were also established.

Keywords: Hydrodynamic; Electroflotation column; Oxygen bubbles; Gas holdup; Viscosity; Surface tension

1. Introduction

Bubble columns are liquid-gas exchanger largely used in industry [1,2]. Several researches approached various aspects within these columns such as mass transfer, heat, and hydrodynamic. In this context, we deal this study with an electroflotation column which is one of bubble columns categories.

In fact, electroflotation is the electrochemical version of traditional dissolved air flotation. It is characterized by its mechanism of oxygen and hydrogen bubble formation due to water electrolysis according to these reactions:

*Anode reaction: water oxidation

$$H_2O \rightarrow \frac{1}{2}O_2 + 2H^+ + 2e^-$$

*Cathode reaction: water reduction

$$2H_2O + 2e^- \rightarrow H_2 + 2OH^-$$

Most of the previous work has shown that the separation efficiency of an electroflotation column depends mainly on both liquid phase physicochemical properties and current density. In this context, L.B Mansour et al. [3–5] highlighted the effect of liquid phase physicochemical property (viscosity, pH, surface tension, density, etc.) on the treatment of wastewaters using electroflotation process. Hosny [6] used insoluble electrodes to separate oil from oil/water emulsions and showed the significant effect of current density on the separation efficiency. Other authors have also shown the importance of current density on the whole process [7,8]. Indeed, the current

*Corresponding author.

density influences directly the number and the size of bubbles [9]. Chen [10] showed that the current density and the mass of bubbles formed are proportional. Pino et al. [11] and other workers [12–15] have also shown that bubble behavior affects in turn the hydrodynamic regime of the separation process. In fact, the high separation efficiency in an electroflotation cell could only be obtained in bubbly laminar regime [16]. Therefore, there is a need to understand the hydrodynamic characteristics in the design of the electroflotation cell used as a column for liquid–solid separation. Hydrodynamic parameters involve particularly the study of bubble shape, bubble rise velocity, Reynolds number, and gas holdup.

In this study, we will inspect the effect of physicochemical characteristics of different model solutions on hydrodynamic parameters and regimes. The method of video recording and image processing was employed in order to determine oxygen bubbles diameters and rise velocities, as well as gas hold up. In fact, studying oxygen bubble characteristics will help us better understand the oxygen transfer phenomenon in the electroflotation bubble column.

In addition to tap water, two types of solution were studied in order to inspect the effect of surface tension and viscosity on the hydrodynamic parameters of the column of electroflotation: a solution of cationic surface tension (CST) and a solution of anionic surface tension (AST).

2. Materials and methods

2.1. Materials

2.1.1. Model solutions characterization

In order to obtain solutions with different physicochemical properties, i.e. with different values of viscosity and surface tension, two model aqueous solutions were prepared in addition to tap water:

- solutions of CST—Benzyl diméthyl *n*-Hexadecyl ammonium chloride,
- solutions of AST—polymethacrylate of Sodium,

All experiments were conducted in ambient conditions (20°C and 1 atm). The physicochemical properties of model solutions are presented in Table 1.

Table 1
Physicochemical properties of model solutions

Solution	Concentration ($g\,l^{-1}$)	Density [$kg\,m^{-3}$]	Surface tension [$N\,m^{-1}$] × 10^{-3}	Viscosity cP
CST	0.1	998.655	66.55	1.11
	0.2	998.441	55.32	1.13
	0.25	998.033	44.87	1.16
	0.3	997.820	40.66	1.2
AST	0.1	997.455	63.48	1.80
	0.25	995.866	68.64	2.17
	0.5	993.144	63.48	2.83
	1	985.176	59.47	5.79
	1.5	983.488	55.45	8.74
	3	979.812	43.4	17.6

2.1.2. Electroflotation column

The measurements were performed in a laboratory-scale electroflotation column using insoluble electrodes. A schematic diagram of the electroflotation column and the equipment for determination of bubble characteristics by image analysis is shown in Fig. 1.

The electroflotation column is made of cylindrical glass vessel and it is of 9.5 cm internal diameter and 1 m in height. It is equipped by titanium coated with ruthenium oxide anode and stainless steel cathode. These two rectangular electrodes (45 mm × 78 mm × 4 mm) are supplied by a generator of DC current (DC Power Supply GPC-M Series from GW-INSTEK-TAIWAN) which makes possible the variation of current density in the electrodes.

A rectangular Plexiglas wall divides the column into two equal compartments. This separation, actually intended to separate the two electrodes, is perforated at the bottom in order to allow the electrolysis reaction to settle. This configuration leads to separate oxygen produced in the anode compartment from hydrogen bubbles produced in the cathode compartment.

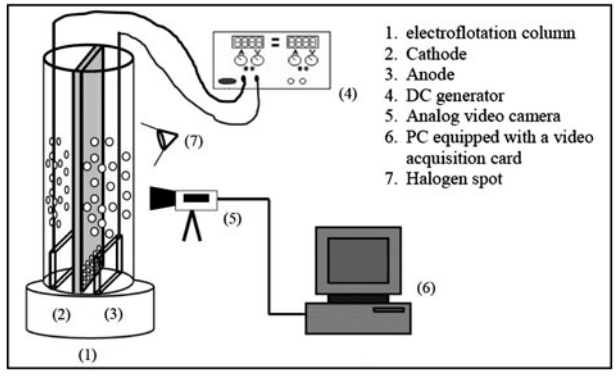

Fig. 1. Electroflotation column and equipment for determination of bubble size distributions.

The equipments used for the determination of the bubble characteristics by image analysis are an analog video camera (model NVA3E from Panasonic, Japan), an acquisition card (model Pinnacle PCTV PRO version 4.02 from Pinnacle systems), a PC with appropriate image analysis software (Photoshop version 7.0 from Adobe, photofiltre 8.0, mesurim pro version 6.0 and Virtual Dub 1.6.11), and a double 50 watt power halogen spots.

2.2. Methods

In order to calculate the average bubble diameter at different operating conditions, images of bubble flow were taken by an analog video camera in each experimental condition. A wire of a known diameter (0.149 mm) was videotaped for use as the calibration factor for the bubble size. Then, we obtain a video file in which the number of frames per second is set. We extract all frames (photos) from this video. We apply a series of filters which lead to clear bubbles as showed. For getting a sufficiently representative bubble size, 50 bubbles were at least measured in each experimental condition. The confidence level for reproducibility of experiments was 95%. The figure below shows bubbles in different current densities applied and for the same liquid phase (Fig. 2).

In addition to the treatment image software, Schafer et al. [17] have shown that good image quality was ameliorated when illuminating the bubbles with diffuse back light. Bubbles then can appear dark on white background (Fig. 3).

During experiments, gas hold up was determined by the bed height method. Gas hold up was calculated using Eq. (1).

Gas hold up:

$$\varepsilon_G = \frac{(H_T - H_S)}{H_T} \quad (1)$$

Fig. 3. Image treated for the determination of bubble size.

where H_T, total height of gas-liquid bed; H_S, the static height of liquid bed.

Bubbles rise velocities were calculated using the Eq. (2) below:

$$U_B = \frac{H}{t} \quad (2)$$

where H is the bubble course in a laps time t. In fact, series of single bubbles were identified and recorded in their ascension. Then, images were treated and superposed in order to calculate the bubble rise velocity. The same wire of known diameter was also used (Fig. 4).

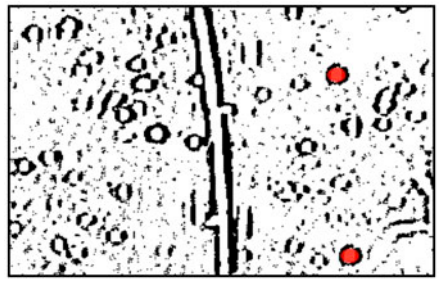

Fig. 4. Images treated and superposed for the determination of bubble rise velocity.

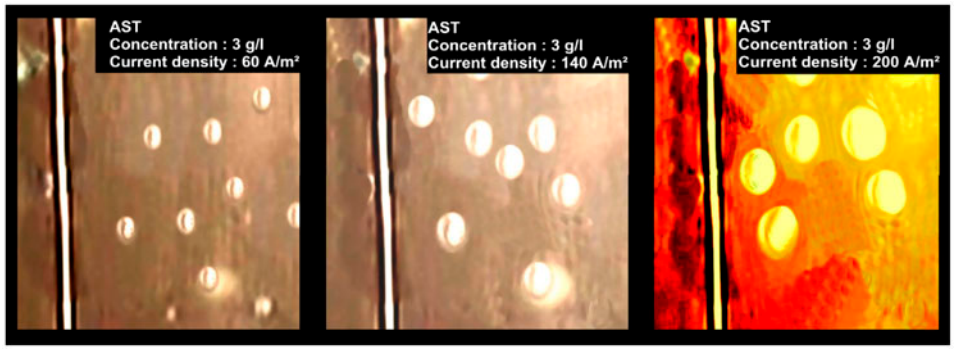

Fig. 2. Bubble size in different current densities applied.

3. Result and discussion

3.1. Effect of surface tension and viscosity on bubble diameter and its rise velocity

In order to check the effect of surface tension and viscosity of liquid phase on both bubble diameter and its rise velocity, experiments were carried out by varying the current density. For CST solution, concentration varied from 0.1 to 0.5 g/l, while it was varied from 0.1 to 3 g/l for the AST solution. The results are shown in Figs. 5–8.

Such remarks can be deduced:

- Whatever the liquid phase characteristics (surface tension or viscosity), increasing current density at the electrodes leads to obtaining larger bubbles which have faster rise velocity. In fact, the effect of current density on bubble size represents a real conflict between researchers. The major affecting parameter is the nature and the configuration of electrodes. For example, smooth-surface electrode and rough-surface electrodes leads to different results [18]. Some authors did not find any effect of current density on bubble size [19]. In our case, bubble is formed at surface of electrodes by taking up gas from the surrounding supersaturated solution. In accordance with Janssen and Hoogland study [20], coalescence between the adhering bubbles at the surface of electrodes is more significant when increasing current density. This justifies that by increasing the current density leads to obtaining larger bubble. However, some authors found the opposite influence [21]. In accordance with our results, Fukuma [22] and Saxena [23] found the same effect on bubble size when increasing gas flow rate. Faraday's law establishes that by increasing the current density leads evidently to an increase of gas flow rate.

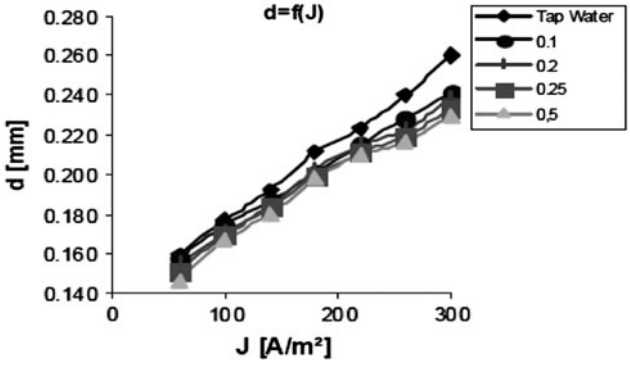

Fig. 5. The variation of bubble diameter with current density: CST solution.

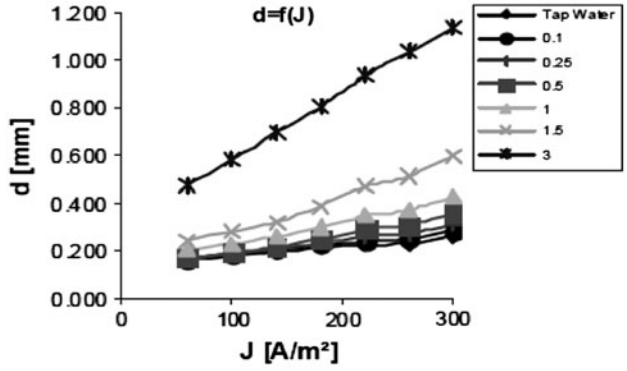

Fig. 6. The variation of bubble diameter with current density: AST solution.

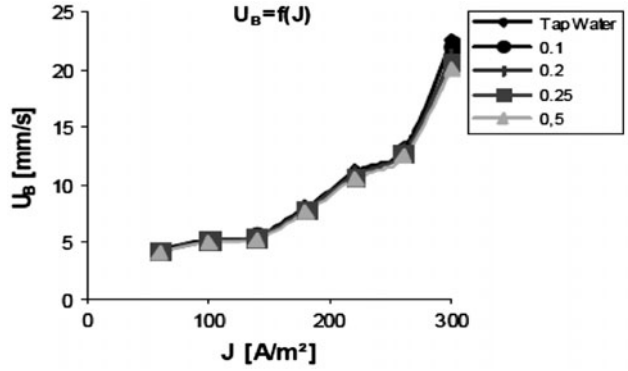

Fig. 7. The variation of bubble rise velocity with current density: CST solution.

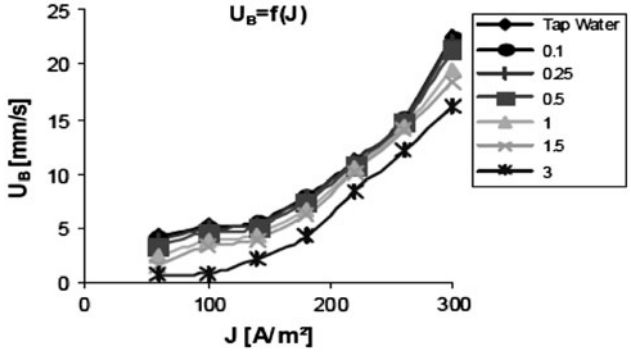

Fig. 8. The variation of bubble rise velocity with current density: AST solution.

$$\dot{m}_G = \frac{I \cdot M_G}{4 \cdot F} \tag{3}$$

where I, amperage [A]; $m_{G,}$ mass flow rate of gas [g s^{-1}]; M_G, Gas molar mass [g mole^{-1}]; F, Faraday constant = 96,485 (C mole^{-1}).

- In case of CST solution we have noticed that the lowest bubble diameters correspond to the most concentrated solutions. That is, by decreasing the solution surface tension contributes to smaller bubbles. These observations agree with Akita work [24]. In case of AST solution, the effect of viscosity is more significant. Indeed, increasing viscosity (higher concentration) leads to an increase of bubble diameter. In fact, increasing liquid viscosity reduces turbulence in the liquid phase. Hence the energy of eddies is reduced and bubble breakage damped, leading to increased bubble sizes [17]. Indeed, as we noted before, bubble is formed at the surface of electrodes by taking up gas from the surrounding supersaturated solution. With our electrodes, increasing viscosity lead to obtaining a greater surrounding supersaturated solution, coalescence between the adhering bubbles at the surface are then more important and lead to obtaining larger bubble diameter. We also noted that bubble size is more affected by varying viscosity than surface tension, larger bubble are obtained in AST solution.
- Concerning bubble rise velocity, we have noticed the same behavior for the two surface active solutions. In fact, increasing the AST or the CST concentration leads to a decrease of bubble rise velocity. Nevertheless, speed falls much more in the case of AST solution because of viscous forces effect. This is justified by the fact that increasing liquid phase viscosity leads to a large increase of drag force (which hampers the bubble to be faster) compared to the other forces (buoyancy force, momentum force, etc.) which help bubbles to be faster. This makes us in the case of biggest and slowest bubble. Then, the increase in viscosity or the decrease in liquid phase surface tension contributes both to a decrease of bubble rise velocity, but with different scale. This decrease is essentially related to the size of bubbles and in all cases, applying a balance of forces on a bubble justifies the effect of surface tension and viscosity on the bubble rise.

Since bubble diameter and bubble rise velocity depend on both liquid phase characteristic (surface tension—viscosity—density) and current density applied at the insoluble electrodes, we have tried to elaborate models using linear regression in order to predict the bubble diameter in case of tap water, CST, and AST solutions:

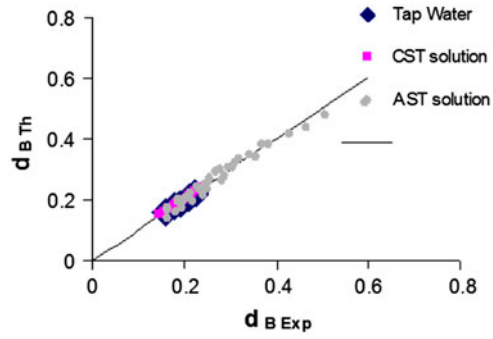

Fig. 9. Comparison between measured ($d_{B\ exp}$) and predicted bubble diameter ($d_{B\ Th}$).

Tap water:

$$d_B = 5.26 \times 10^{-2} \times J^{0.267} \quad (4)$$

$$U_B = 8.84 \times 10^{-2} \times J^{0.881} \quad (5)$$

CST solution:

$$d_B = 1.02 \times 10^{-2} \times J^{0.275} \times \rho^{0.393} \times \sigma^{0.097} \times \mu^{0.128} \quad (6)$$

$$U_B = 2.45 \times 10^{-3} \times J^{1.125} \times \rho^{0.207} \times \sigma^{0.057} \times \mu^{-0.158} \quad (7)$$

AST solution:

$$d_B = 9.64 \times 10^{-3} \times J^{0.44} \times \rho^{0.493} \times \sigma^{0.103} \times \mu^{0.358} \quad (8)$$

$$U_B = 1.3 \times 10^{-3} \times J^{1.698} \times \rho^{0.133} \times \sigma^{0.413} \times \mu^{-0.017} \quad (9)$$

where d_B, bubble diameter [mm]; ρ, liquid phase density [kg m^{-3}]; J, current density [A m^{-2}]; σ, liquid phase surface tension [N m^{-1}]; U_B, Bubble rise velocity [mm s^{-1}]; μ, liquid phase viscosity [kg m^{-1} s^{-1}].

We give in the figure below a comparison between measured and predicted bubble diameter. (Fig. 9)

3.2. Effect of surface tension and viscosity on gas holdup and specific interfacial area

As shown in Figs. 10 and 11, experiments were also conducted by varying current density at the electrodes in order to determine gas holdup using the bed height method. Indeed, gas holdup is a parameter used in the calculation of the specific interfacial area (a) which is an important parameter in the characterization of the transfer phenomenon in the column [25]:

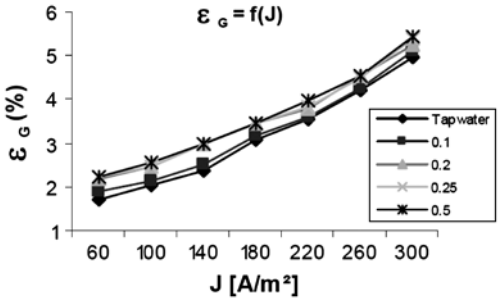

Fig. 10. The variation of gas holdup with current density: CST solution.

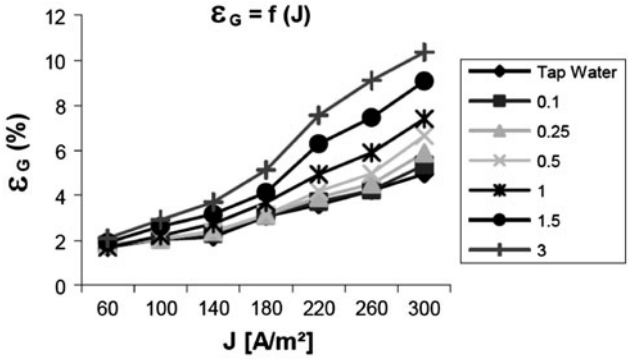

Fig. 11. The variation of gas holdup with current density: AST solution.

$$a = \frac{6 \times \varepsilon_G}{d_B \times (1 - \varepsilon_G)} \tag{10}$$

Concerning gas holdup, we have noticed that:

- For all model solutions, when current density increases, gas holdup also increases.
- When surface tension of solution decreases (by adding the CST agent) or when viscosity increases (by adding the AST agent), we notice that gas holdup increases. It is also noted that viscosity has a great effect on gas holdup than surface tension.
- The higher values of gas holdup are obtained in AST solution which means that the viscosity has a more significant effect on gas holdup.
- Models were also established in order to predict gas holdup variation using linear regression method:

In case of tap water:

$$\varepsilon_G = 7.11 \times 10^{-4} \times J^{0.73} \tag{11}$$

In case of CST solution:

$$\varepsilon_G = 0.89 \times J^{0.57} \times \rho^{0.66} \times \sigma^{0.14} \times \mu^{1.53} \tag{12}$$

In case of AST solution

$$\varepsilon_G = 3.89 \times 10^{-4} \times J^{1.13} \times \rho^{0.36} \times \sigma^{0.70} \times \mu^{0.31} \tag{13}$$

These models agree with Reilly work [26]. In fact, gas holdup depends mainly on both liquid phase physicochemical properties and gas properties (bubble size and velocity) which are related to current density in our work.

Concerning specific interfacial area, we have noted that electroflotation method leads to obtaining the high values of specific interfacial area (a) ($\approx$600 mm^2 / mm^3) compared to other bubble generation processes [27]. We have also noticed that high specific interfacial area can be obtained by increasing current density,

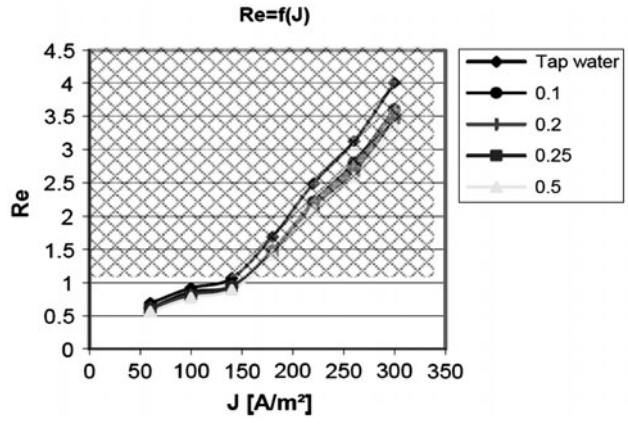

Fig. 12. The variation of Reynolds number with current density: CST solution.

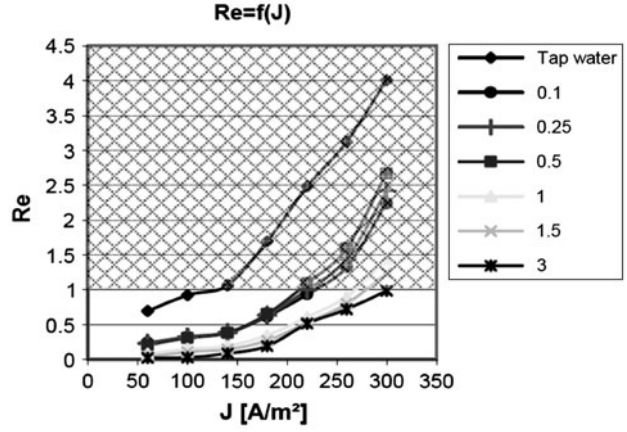

Fig. 13. The variation of Reynolds number with current density: AST solution.

Table 2
Models predicting the variation of Reynolds for each solution

Tap water	$\mathrm{Re} = 8.566 \times 10^{-3} \times J^{0.694} + 0.3 \times d_B^{1.954} + 0.084 \times U_B^{1.307} - 0.043$
CST solution	$\mathrm{Re} = 5.429 \times 10^{-3} \times J^{0.7} + 0.3 \times d_B^{1.955} + 0.069 \times U_B^{1.345} + 0.014$
AST solution	AST concentration ($0.1 \rightarrow 0.5\,g/l$)
	$\mathrm{Re} = 5.80 \times 10^{-6} \times J^{0.289} + 2.61 \times 10^{-6} \times d_B^{0.102} + 0.092 \times U_B^{1.155} - 0.435 \times \mu_L^{0.162} + 0.056$
	AST concentration ($1 \rightarrow 3\,g/l$):
	$\mathrm{Re} = 2.56 \times 10^{-4} \times J^{0.4} + 0.116 \times d_B^{0.22} + 2.41 \times 10^{-2} \times U_B^{1.345} - 0.163 \times \mu_L^{0.129} - 0.113$

Where J [A/m²]—d_B [mm]—U_B [mm/s]—μ_L [kg m^{-1} s^{-1}].

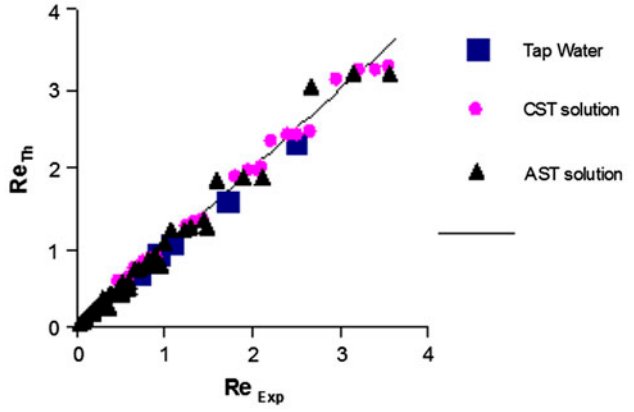

Fig. 14. Comparison between measured (Re $_{exp}$) and predicted (Re $_{Th}$) Reynolds number.

increasing viscosity, or decreasing surface tension of liquid phase.

3.2. Analysis of the hydrodynamic regimes

In case of gas–liquid flow, it is known that transition from laminar to turbulent flow can be achieved by the calculation of Reynolds number $\mathrm{Re} = \frac{\rho_L \times V_B \times d_B}{\mu_L}$. The value Re = 1 delimits this zone [28].

For the three types of the studied solutions (tap water, CST, and AST solution), this number was calculated. The Figs. 12 and 13 show the variation of Reynolds number in each case according to the current density applied to the electrodes.

We note that:

- The transition from laminar to turbulent flow is obtained with a current density of 140 A/m² in case of tap water.
- In case of CST solution, the transition is little moved to higher current density value (150 A/m²). In fact, compatible with previous researches [24], when surface tension decreases, the bubble size and its rise velocity also decreases. This explains well that the Reynolds numbers also decreases.
- In case of AST solution, the transition is significantly moved to higher current density value (>200 A/m²). In fact, when viscosity increases, the size of bubbles increases significantly which leads to a drop of their velocities. In other words, the viscous forces dominate momentum, buoyant, or gravitational forces and we need more energy to reach turbulent regime.
- Models predicting the variation of Reynolds numbers were established in each case using linear regression method (Table 2).

This last figure gives a comparison between measured and predicted Reynolds number (Fig. 14).

4. Conclusion

An electroflotation column was used in order to study the hydrodynamic of bubbles. The method of video recording and image treatment was adopted. Model solutions (CAST and AST solutions) and tap water were used in order to check the effect of both liquid phase physicochemical characteristics and current density on bubbles diameter characteristics, and gas hold up. We have noticed that smaller bubbles are obtained by decreasing the solution surface tension or decreasing viscosity. Whereas, increasing viscosity or decreasing liquid phase surface tension contributes to a decrease of bubble rise velocity. In the other hand, the viscosity has also a significant effect on gas holdup more than liquid phase surface tension. In fact, decreasing surface tension or increasing viscosity leads to an increase of gas holdup.

An analysis of hydrodynamic regimes was also established by calculating Reynolds numbers. We found that both current density and liquid phase viscosity has a significant effect on the transition from laminar to turbulent flow. Models predicting the variation of Reynolds numbers were established in each case using linear regression method.

Symbols

CST — cationic surface tension, Benzyl diméthyl *n*-Hexadecyl ammonium chloride
AST — anionic surface tension, polymethacrylate of Sodium
ε_G — gas hold up, –
H_T — total height of gas-liquid bed, L
H_S — static height of liquid bed, L
U_B — bubbles rise velocity, $L\,T^{-1}$
d_B — bubble diameter, L
ρ — liquid phase density, $M\,L^{-3}$
J — current density, $A\,L^{-2}$
σ — liquid phase surface tension, $M\,T^{-2}$
μ — liquid phase viscosity, $M\,L^{-1}\,s^{-1}$
a — specific interfacial area, $L^3\,L^{-2}$
Re — Reynolds number, –

References

[1] F.P. Shariati, B. Bonakdarpour, M.R. Mehrnia, Hydrodynamics and oxygen transfer behaviour of water in diesel microemulsions in a draft tube airlift bioreactor, Chem. Eng. Process 46 (2007) 334–342.
[2] D. Ghernaouta, M.W. Naceura, B. Ghernaoutb, A review of electrocoagulation as a promising coagulation process for improved organic and inorganic matters removal by electrophoresis and electroflotation, Desalin. Water Treat. 28 (2011) 287–320.
[3] L. Ben Mansour, Y. Ben Abdou, S. Gabsi, Effects of some parameters on removal process of nickel by electroflotation, Water Waste Environ. Res. 2 (2001) 51–58.
[4] L. Ben Mansour, I. Kesentini, Treatment of effluents from cardboard industry by coagulation-electroflotation, J. Hazard. Mater. 153 (2008) 1067–1070.
[5] I. Ksentini, M.L. Aouadi, H. Ben Bacha, L. Ben Mansour, Solar energy integration in the treatment of industrial effluent by coagulation–electroflotation, Desalin. Water Treat. 20 (2010) 60–65.
[6] A.Y. Hosny, Separation of oil from oil/water emulsions using an electroflotation cell with insoluble electrodes, Filtr. Sep. J. 29(5) (1992) 419–423.
[7] V.A. Kolesnikov, S.O. Varaksin, V.I. Ilyin, An electroflotation method for purifying effluents from ions of metals and organic pollutants and its equipment, Russ. Chem. Ind. 26 (1994) 38–46.
[8] M. Murugananthan, G. Bhaskar Raju, S. Prabhakar, Separation of pollutants from tannery effluents by electroflotation, Sep. Purif. Technol. 40 (2004) 69–75.
[9] Y. Fukui, S. Yuu, Removal of colloidal particles in electroflotation, AIChE J. 31(2) (1985) 201–208.
[10] G. Chen, Electrochemical technologies in waste water treatment, Sep. Purif. Technol. 38 (2004) 11–41.
[11] L.Z. Pino, M.M. Yepez, A.E. Saez, An experimental study of gas holdup in two-phase bubble columns with foaming liquids, Chem. Eng. Commun. 89 (1990) 155–157.
[12] Y.T. Shah, S. Joseph, D.N. Smith, J.A. Ruether, On the behavior of the gas phase in a bubble column with ethanol–water mixtures, Ind. Eng. Chem. Process 24(4) (1985) 1140–1148.
[13] R. Pohoreski, W. Moniuk, Zdrojkowski Hydrodynamics of a bubble column under elevated pressure, Chem. Eng. Sci. 54 (1999) 5187–5193.
[14] K. Idogawa, K. Ikeda, F. Fukuda, S. Morooka, Behaviour of bubbles of the air–water system in a column under high pressure, Int. Chem. Eng. 26 (1986) 468–474.
[15] T.J. Lin, K. Tsushiya, L.S. Fan, Bubble flow characteristics in bubble columns at elevated pressure and temperature, AIChE. J. 44 (1998) 545–560.
[16] L. Ben Mansour, S. Chalbi, I. Kesentini, Experimental study of hydrodynamic and bubble size distributions in electroflotation process, Ind. J. Chem. Tech. 14 (2007) 253–257.
[17] R. Schafer, C. Merten, G. Eigenberger, Bubble size distributions in a bubble column reactor under industrial conditions, Exp. Therm. Fluid Sci. 26 (2002) 595–604.
[18] D. Lumanauw, Hydrogen bubble characterization in alkaline water electrolysis. MSc thesis, Department of Metallurgy and Materials Science, University of Toronto, Canada, 2000.
[19] S.E. Burns, S. Yiacoumi, C. Tsouris, Microbubble generation for environmental and industrial separations, Sep. Purif. Technol. 11(3) (1997) 221–232.
[20] L.J.J. Janssen, J.G. Hoogland, The effect of electrolytically evolved gas bubbles on the thcikness of the diffusion layer, Electrochim. Acta 15 (1970) 1013–1023.
[21] D.R. Ketkar, R. Mallikarjunan, S. Venkatachalam, Size determination of electrogenerated gas bubbles, J. Electrochem. Soc. India 37(4) (1988) 313–318.
[22] M. Fukuma, K. Muroyama, S. Morooka, Properties of bubble swarm in a slurry bubble column, J. Chem. Eng. Jpn. 20 (1987) 28–33.
[23] S.C. Saxena, N.S. Rao, A.C. Saxena, Heat-transfer and gas-holdup studies in a bubble column: Air–water–glass bead system, Chem. Eng. Commun. 96 (1990) 31–55.
[24] K. Akita, F. Yoshida, Bubble size interfacial area, and liquid-phase mass transfer coefficient in bubble columns, Ind. Eng. Chem. Process Des. Dev. 13(1) (1974) 84–91.
[25] R. Maceiras, E. Álvarez, M.A. Cancela, Experimental interfacial area measurements in a bubble column, Chem. Eng. J. 163(3) (2010) 331–336.
[26] I.G. Reilly, D.S. de Scott, T.J.W. Bruijn, A. Jain, J. Piskorz, A correlation for gas holdup in turbulent coalescing bubble columns, Can. J. Chem. Eng. 64 (1986) 705–717.
[27] Pisut Painmanakul, Analyse locale du transfert de matière associé à la formation de bulles générées par différents types d'orifices dans différentes phases liquides Newtoniennes: étude expérimentale et modélisation [Local analysis of mass transfer associated with the formation of bubbles generated by different types of orifices in different Newtonian liquid phases: Experimental study and modeling], PhD thesis, INSA de TOULOUSE, 2005.
[28] A.A. Kendoush, T.J. Mohammed, B.A. Abid, M.S. Hameed, Experimental investigation of the hydrodynamic interaction in bubbly two-phase flow, Chem. Eng. Process 43 (2004) 23–33.